TÜBİTAK

Turkish Journal of Physics

http://journals.tubitak.gov.tr/physics/

Review Article

Turk J Phys
(2018) 42: 89 – 96
© TÜBİTAK
doi:10.3906/fiz-1711-13

Characterizing decaying dark matter: X-ray emission from sterile neutrinos

Murat HÜDAVERDİ*
Department of Physics, Faculty of Science and Art, Yıldız Technical University, İstanbul, Turkey

Received: 15.11.2017 • **Accepted/Published Online:** 16.01.2018 • **Final Version:** 13.02.2018

Abstract: Recently, an unknown emission line at E ∼3.5 keV from several astrophysical objects has been detected. The line is suggested to be originating from decaying dark matter particles. The results have drawn great attention from the astrophysics and particle physics community. Since the detected line is significantly weak there has also been a long debate over the origin of this mysterious signal. The most accepted scenario is a radiatively decaying sterile neutrino of 7.1 keV in mass producing a monochromatic 3.5 keV line, which is observable in X-ray energy ranges. The problem has not been settled and further observations from more objects are needed to verify the detection in order to constrain the physical properties and the nature of the signal. In this paper, we present the current situation and provide further insights into the subject.

Key words: X-ray, emission lines, dark matter, sterile neutrinos

1. Introduction

In 1937, Fritz Zwicky studied velocity dispersion as a function of radius for the Coma Cluster of galaxies [1]. He noticed something strange about the way they moved. The galaxies were going too fast (around 1000 km s^{-1}), so fast that they should have been flying apart. The mass of the visible material, the stars and all those galaxies inside, had too little gravitational potential to hold the Coma system together. Zwicky though that something else must be binding the matter together. He was the first astronomer to postulate that the clusters must contain a lot of an invisible form of material, dark matter. The scientific community did not pay much attention to this wild notion of the universe at his time. About 30 years later, Vera Rubin studied the Andromeda galaxy and discovered that the outer stars move at the same speed as the closer ones [2]. This was unusual and unexpected by the law of gravity. However, following studies showed that it was not only Andromeda; 60 other galaxies were also violating the known physics. These observations supported Zwicky's idea of dark matter that there was something massive and invisible, which was forcing the stars to go fast. Other evidence for the existence of dark matter includes galactic rotation curves, gravitational lensing [3], cosmic microwave background radiation, and extended hot gas in clusters of galaxies. The existence of dark matter is inevitable for today's cosmology. Most of the matter in the universe is composed of this new but indefinite form of building blocks. Instead of inducing a new mysterious form of matter, a group of researchers also tried to explain some observed effects by adjusting the theory of gravity. A modified Newtonian dynamics (MOND) was postulated as an alternative theory [4]. However, MOND itself cannot explain observations on all scales without any dark matter [5].

Explaining dark matter in terms of new particles requires further physics and pushes the edges of the

*Correspondence: hudaverd@yildiz.edu.tr

standard model. One of the first proposed viable candidates for dark matter came from massive astrophysical compact halo objects, or "MACHOs" [6, 7]. They were claimed to be discovered by the gravitational lensing mechanism. These objects are black holes, neutron stars, or brown dwarfs, in which matter is in the form of dense chunks of heavy elements. However, we now know it is unlikely that enough MACHOs could pile up to form the vast amount of dark matter that exists [8]. In fact, there is a group of very successful dark matter candidates of heavy particles with masses above the electroweak scale, which are called weakly interacting massive particles (WIMPs) [9]. WIMPs are divided into three subgroups as cold, warm, and hot dark matter. Here the definitions refer to the particle's mobility rather than its temperature. The velocity of the particle decides how far it can travel in a definite time. The distance traveled by a particle before it is slowed down by cosmic expansion is called its free-streaming-length (FSL). In order to explain the current picture of the cosmos, particles with different mobilities have been checked for agreement. There are suggestions providing a variety of suitable dark matter particles, but there is no clear evidence telling us which of these is correct. While many studies are being conducted and collecting data, no conclusive evidence for WIMPs has yet been reported.

If WIMPs are defined to be cold (slow) and collisionless, the FSL will be much smaller than the galaxy scale. In this cold dark matter (CDM) scenario, the particles move so slowly that the formation of small-scale structures can not be smoothed out, i.e. dwarf galaxies. Thus, CDM suggests that smaller objects form first and then merge into larger structures in a bottom-up fashion (e.g., [10, 11]). This cosmology elegantly explains structural formation on big scales but includes several unresolved problems. Advanced simulations reveal some disagreement between purely CDM scenarios and observations on small scales ($\sim$10 kpc) [12]. The number of dwarf galaxies is expected to be very high in this cosmology, since CDM particles are very slow and can not wash out small entities. However, this is not supported by the observations, which is known as the missing satellite problem [13]. A similar problem occurs in density profiles of galaxies. The simulations estimate a cusp profile at r $\leq$ 10 kpc [14]. Several solutions are proposed, such as supernova and AGN feedbacks [15, 16]. The solutions from these type of baryonic contents are found to be doubtful because it is just a minor component of galaxies.

Dark matter particles with a large velocity dispersion are called hot dark matter (HDM). In this cosmology, the particles can travel longer distances and their FSL would be larger than a galaxy scale. HDM particles are so energetic and fast, all possible galaxy-size small cosmic fluctuations are expected to be smoothed out. Therefore, the existence of small-scale structures like protogalaxies is inexplicable in this cosmology. The HDM scenario suggests that larger structures like clusters form first, then are broken into smaller galaxies in a top-down fashion [17].

If the particles are adjusted to preserve the small-scale fluctuations in the expected range, we can better explain the observed universe. In order to reduce the discrepancy, the particles are assumed to be warmer than CDM and cooler than HDM. These particles are called warm dark matter (WDM), which have a FSL comparable to the galaxy scales [18]. In the WDM cosmology, the number of dwarf galaxies and the amount of dark matter in the galaxy centers are expected to be less than in the CDM. On large scales, both cosmologies predict similar results. While the disagreement between simulations and observations is evident, the dark matter origin is not clear yet. Furthermore, dark matter may be not purely cold, warm, or hot, but a mixture of all in a more complicated diverse model [19].

Based on experiments, theory, and observations, the constraints for dark matter are coming from all disciplines and perspectives: particle physics, cosmology, and astrophysics. The recent observational evidence from several astrophysical objects has drawn great attention from the scientific community. Researchers found

indications for an unidentified emission line at E ∼3.5 keV in the X-ray spectra of various objects. The signal was detected at 73 stacked clusters [20], the Perseus cluster center [20, 21] and outskirts [22], Andromeda [22], and the Milky Way [23, 24]. The measurements were performed by using different detectors (*Chandra*, *XMM-Newton*, and *Suzaku*), which significantly ruled out instrumental uncertainties. However, a number of studies tend to reject the presence of such a signal and try to explain it with the coupling of the neighboring emission lines (e.g., [25]). Nevertheless, a 7.1 keV mass of sterile neutrino, which decays into an X-ray photon of energy $E_\gamma = m_s/2$ and an active neutrino, is widely accepted. The dark matter candidate in the keV mass range also seems feasible for WDM cosmology [26]. For more than a decade *Chandra*, *XMM-Newton*, and *Suzaku* are piling up a vast collection of archival data. Searching these databases can give rise to statistical and systematic uncertainties.

2. X-ray spectrum around 3.55 keV

Modeling an unknown emission line is challenging because the X-ray spectra of astrophysical sources are crowded with various emission lines. Strong neighboring signals can easily hide and artificially smooth out any weak line feature in the data. In order to identify an unknown line emission, one should pinpoint all the well-known emission lines.

There are strong Ne `X` (1.21 keV), Fe `XXIV` (1.55 keV), Mg `XII` (1.74 keV), and Si `XVII` (1.86 keV) lines below 2 keV. Around these energies any detection is very challenging. Thankfully, the lower bound of the expected line emission from a dark matter candidate is 2.0–2.5 keV, which is constrained from the Lyman-α forests (e.g., [27, 28]) (see Section 3 for details). Thus, spectral analysis has been performed above E $>$ 2 keV. The strong emission from extend plasma includes about 30 lines between the 2 and 10 keV bands as listed in the Table. Besides the astrophysical lines, there are also instrumental lines such as Al-K (1.49 keV), Si-K (1.74 keV), Ni-K (7.48 keV), Cu-K (8.05, 8.91 keV), and Zn-K (8.64, 9.57 keV).

Limiting the spectral fitting between the 3 and 4 keV energy bands, Ar `XVII`, K `XVIII`, and Ca `XIX` lines (see the Table) has to be carefully modeled. Figure 1 shows the locations of the emission lines in the 3–4 keV band (adapted from [20]). The black arrow indicates 3.55 keV energy. The figure also visually highlights the potential risk of contamination from Ar `XVII`, K `XVIII`, or Ca `XIX` lines. During the spectral analysis, all physical and instrumental lines have to be modeled by respective Gaussian lines, since all above mentioned signals are treated as background as we focus on 3.55 keV emission.

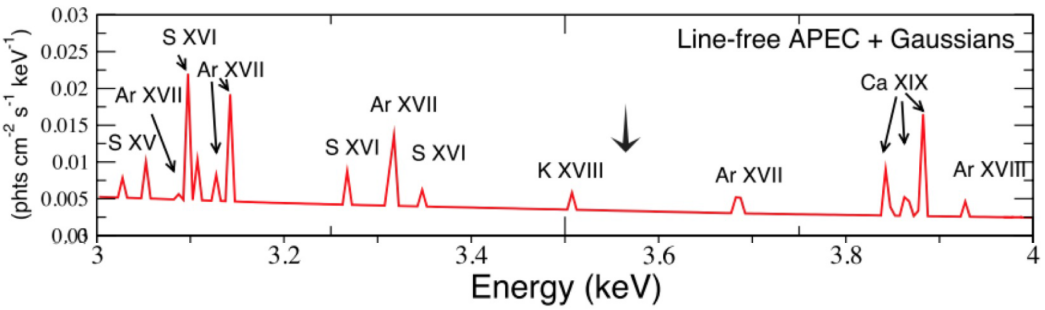

Figure 1. Emission lines in the 3–4 keV range. Black arrow indicates the location of 3.55 keV [20].

Table. List of known emission lines between 2 and 10 keV bands.

Energy [keV]	Line	Energy [keV]	Line	Energy [keV]	Line
2.01	Si XIV	3.47	K XVIII	6.39	Fe K-α
2.05	Al XIII	3.51	K XVIII	6.62	Fe XXIV
2.18	Si XII	3.62	Ar XVII	6.95	Fe XXIV
2.29	Si XII	3.68	Ar XVII	6.70	Fe XXV
2.34	Si XII	3.71	K XIX	7.29	Fe XXV
2.45	Si XV	3.86	Ca XIX	7.79	Ni XXVII
2.51	Si XIV	3.90	Ca XIX	7.81	Fe XXV
2.62	Si XIV	3.93	Ar XVIII	7.88	Fe XXV
2.88	Si XV	4.10	Ca XX	8.29	Fe XXV
3.12	Ar XVII	4.58	Ca XIX	8.30	Fe XXVI
3.31	Ar XVIII	5.69	Ca XXIII	8.70	Fe XXVI

3. Sterile neutrinos in cosmology

The sterile neutrino mass range and the magnitude have a powerful effect on the resulting cosmology. Different mass scales could explain different astrophysical events and establish boundaries for the physically acceptable range. A lower boundary is obtained from the phase-space density of dwarf galaxies, which is well known as the Tremaine–Gunn bound [29], and gives a sterile neutrino mass of $m_s \geq 0.4$ keV [19]. Another strong lower boundary is derived by measurements of the Lyman-α forests (e.g., [27, 28]). The observations suggest a mass bigger than $m_s > 2.5$ keV. The left panel of Figure 2 shows the lower limit on the sterile-neutrino mass by the Tremaine–Gunn bound in purple, the Fornax dwarf spheroidal galaxy with a shaded area [30], and various upper limits from clusters, the Milky Way, and CMB with different colors. Recent observations show that a sterile neutrino with a keV mass range is more favorable.

Sterile neutrinos can mix with active neutrinos and decay on very long timescales, such as longer than the age of the universe [24]. An upper bound comes from the mixing angle of the particle's lifetime [31] (See Figure 2, right panel). The mixing angle for one-loop radiative decay is given by [32]

$$\theta^2 < 1.1 \times 10^{-7} \left(\frac{50 \text{ keV}}{m_s} \right). \tag{1}$$

If the sterile neutrino is produced by mixing with active neutrinos, the mass should be less than $m_s < 50$ keV [33, 34]. Therefore, the mass of dark matter sterile neutrinos should be in the range of 2.5–50 keV. The constraints are discussed extensively in recent reviews (e.g., [32, 35]). The readers may refer to Klasen et al. [36] for more information.

4. Sterile neutrinos from X-ray sources

In 2014, an unidentified 3.55 keV emission line was detected from the X-ray observations of 73 stacked galaxy clusters [20], and a week later in the Andromeda (M31) and the Perseus galaxy cluster by an independent group [20, 22]. Figure 3 shows the spectra of the Perseus Cluster in the 3–4 keV range with two different telescopes. The red dots show the location of the 3.55 keV residual before the Gaussian component is added to the spectra. The blue circles show the improvement of the spectral fit after adding a narrow Gaussian line. The signal is detected from two different observatories (*XMM-Newton* and *Chandra*) and different detectors (MOSs, PN, ACIS-I, and ACIS-S), which rules out instrumental artifacts. The possibility of this indirect detection of dark

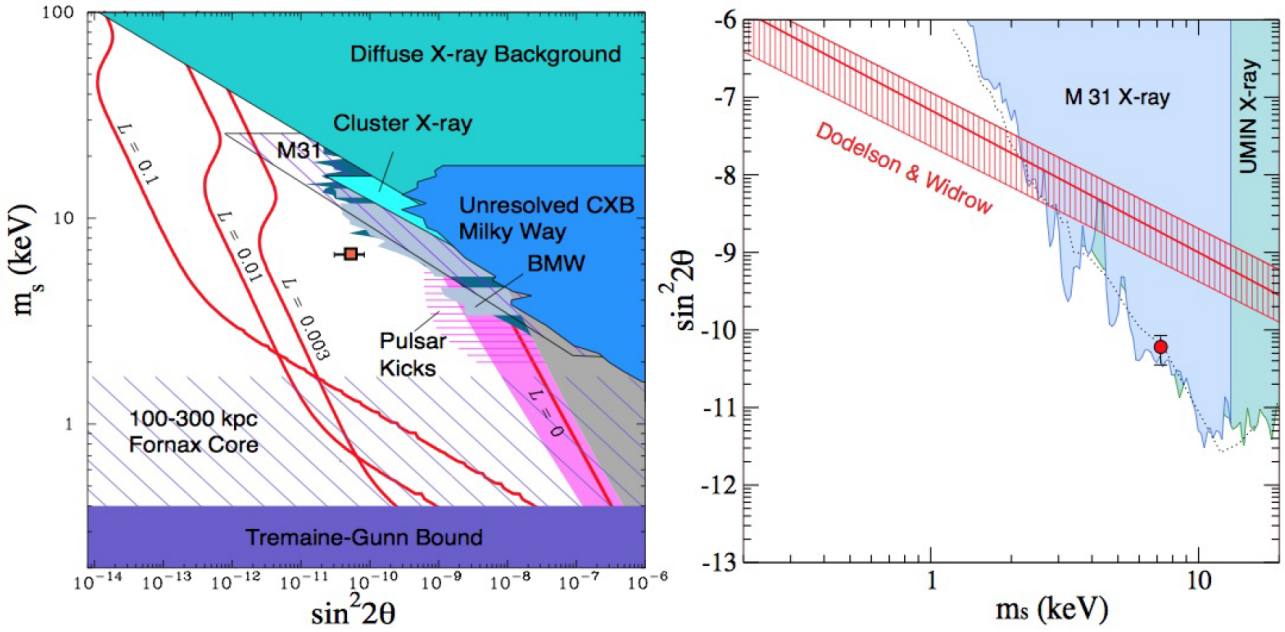

Figure 2. Current constraints on mixing angle and sterile neutrino mass (image credit: Bulbul et al. [20]). Red square shows reported 3.55 keV emission due to decay of sterile neutrino. The colored area is forbidden values by various X-ray emissions (sources are written). The constraints are discussed extensively in recent reviews (e.g., [32, 35]). Red lines are various lepton numbers for the Dodelson–Widrow scenario [26]. See [36] for more information.

matter particles excited the community and received great attention.

The nondetection of the line from Milky Way [37] and the diffuse X-ray background [22, 23] are also valuable, as they brought an upper bound to the solutions. Figure 2 also shows observational constraints on sterile neutrino mass and mixing angle. Different colors represent the constraints from different X-ray objects. Red lines denote various lepton numbers as indicated. The Dodelson–Widrow band [26] is shown with a red-hatched line ($L = 0$) in the right panel.

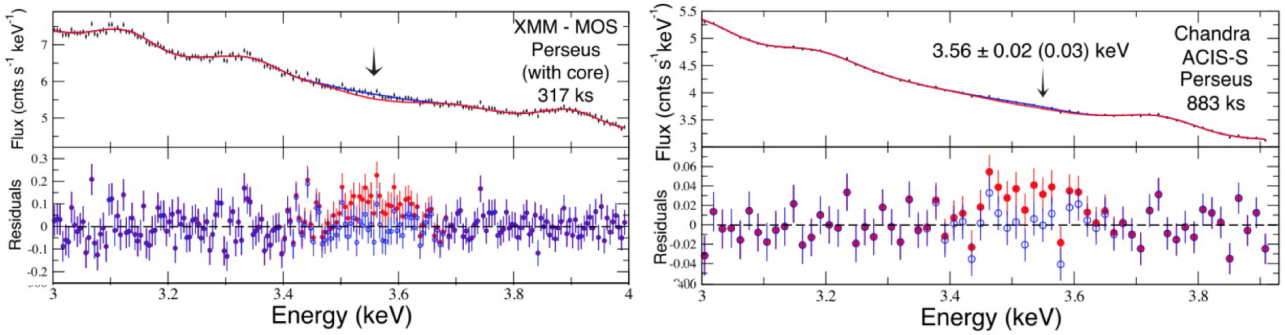

Figure 3. Detection of 3.55 keV emission line obtained from *XMM-Newton* (left) and *Chandra* (right) observations of the Perseus cluster [20]. Red data points are before and blue circles are after a Gaussian component is added.

5. Radiative decay of dark matter

An appealing interpretation of the line is radiative decay of a sterile neutrino as a dark matter candidate [38]. If the majority of dark matter is in the form of a sterile neutrino, the radiative decay can induce a detectable emission, which can be observed in the X-ray band [31]. Nevertheless, the sterile neutrino dark matter is not quite stable. It decays into a neutrino and a photon $N \rightarrow \nu + \gamma$, which produces the detected monochromatic X-ray line [32]. The dark matter particles with mass m_s decay into an active neutrino and emit photons at the energy $E_\gamma = m_s/2$. The flux of this emission is

$$F = \frac{\Gamma\ M_{\rm DM}^{fov}}{4\pi d^2\ m_s}, \tag{2}$$

where $M_{\rm DM}^{fov}$ is the total dark matter mass within the field of view. The decay rate Γ is then given by the mixing angle θ and the sterile neutrino mass m_s according to the following relation [39, 40]:

$$\Gamma = \frac{9\ \alpha\ G_{\rm F}^2}{256 \cdot 4\pi^4} sin^2(2\theta)\ m_s^5 = 1.38 \times 10^{-22}\ sin^2(2\theta)\ \left[\frac{m_s}{1\ keV}\right]^5\ s^{-1}, \tag{3}$$

where $\alpha = 1/137.0$ and $G_{\rm F} = 1.2\ \times 10^{-5}\ {\rm GeV}^{-2}$. In the literature, $\sin^2(2\theta)$ is traditionally called the mixing angle instead of θ. The first ever decay of dark matter is expected to be emitted from the diffuse X-ray background [31, 41]. The dark matter decay contribution to the X-ray background flux is given by [42]

$$F_{\rm XRB} \simeq \frac{\Gamma_{N\rightarrow\ \gamma\ \nu_\alpha}\ \rho_{\rm DM}^0}{2\pi\ H_0} \simeq 8 \times 10^{-11} \left[\frac{\theta^2}{10^{-11}}\right] \left[\frac{m_s}{7\ keV}\right]^5\ \frac{erg}{cm^2 \cdot s \cdot sr}\ , \tag{4}$$

where $\rho_{\rm DM}^0$ and H_0 are the dark matter density and the Hubble constant today. The nondetection of dark matter decay in the X-ray background allows us to constrain a bound on $\sin^2(2\theta)$ and m_s with a function of [42]

$$\text{XRB bound: } \Omega_s\ sin^2(2\theta) \leq\ 3 \times 10^{-5}\ \left[\frac{1\ keV}{m_s}\right]^5, \tag{5}$$

where Ω_s is the present-day density of the sterile neutrino dark matter. The dark matter signal is also expected to be strong in the direction of large mass concentrations, such as galaxy clusters. An estimate of dark matter decay from a galaxy cluster is [41]

$$F_{\rm cluster} \simeq \frac{\Gamma_{N\rightarrow\ \gamma\ \nu_\alpha}\ M_{\rm DM}}{4\pi D_L^2 m_s} \simeq 1.4 \times 10^{-7} \left[\frac{\theta^2}{10^{-11}}\right] \left[\frac{m_s}{7\ keV}\right]^4 \left[\frac{D_L}{100\ Mpc}\right]^{-2} \left[\frac{M_{\rm DM}}{10^{13}\ M_\odot}\right]^{-2} \frac{ph}{cm^2 \cdot s}, \tag{6}$$

where $M_{\rm DM}$ is the dark matter mass within the field of view and D_L is the luminosity distance. Nearby dark matter concentrations like the dwarf spheroidal (dSph) have much smaller dark matter masses. The decay line is in orders of magnitude lower than clusters [43].

$$F_{\rm dSph} \simeq 1.4 \times 10^{-7} \left[\frac{\theta^2}{10^{-11}}\right] \left[\frac{m_s}{7\ keV}\right]^4 \left[\frac{D_L}{100\ Mpc}\right]^{-2} \left[\frac{M_{\rm DM}}{10^7\ M_\odot}\right]^{-2} \frac{ph}{cm^2 \cdot s}. \tag{7}$$

Finally, the nearest dark matter reservoir is the Milky Way, expected to produce dark matter signals comparable to galaxy clusters and dSph galaxies [42].

Most of the attempts to detect dark matter decay in X-rays do not succeed in finding the line. Nondetection works are also valuable as they compel the upper limit on the dark matter sterile neutrino mixing angle as a function of the mass. Some of these limits are shown in Figure 2.

In addition to the 3.55 keV line, other potential lines as radiative decay have also been proposed. Based on the *Suzaku* observation of the Milky Way center a signal has been detected at 8.7 keV [44], and an alternative sterile neutrino is proposed with mass $m_s = 17.4$ keV. If dark matter is not solely composed of a single type of sterile neutrino, it could be composed of a delicate mixture from both 7.1 keV and 17.4 keV mass sterile neutrinos. An alternative scenario proposes 80% of dark matter being 7.1 keV sterile neutrinos and 20% of dark matter being 17.4 keV sterile neutrinos, satisfying the observed cosmology [45].

6. Conclusion

In this paper, we provide an up-to-date review of keV scale sterile neutrinos as dark matter candidate particles. Based on the astrophysical observations, sterile neutrinos could indeed describe the detected unknown X-ray signal. Although well established by indirect evidence, the properties and nature of dark matter still remain a mystery. Further verification can be done by next-generation X-ray observations.

Acknowledgments

We would like to acknowledge financial support from the Scientific and Technological Research Council of Turkey (TÜBİTAK), project number 115F030. The work was also supported by YTU Scientific Research & Project Office (BAP) funding with contract number 2015-01-01-KAP05.

References

[1] Zwicky, F. *Astrophys. J.* **1937**, *86*, 217-246.

[2] Rubin, V. C.; Ford, W. K. *Astrophys. J.* **1970**, *159*, 379-404.

[3] Clowe, D.; Bradač, M.; Gonzalez, A. H.; Markevitch, M.; Randall, S. W.; Jones, C.; Zaritsky, D. *Astrophys. J. Lett.* **2006**, *648*, L109-L113.

[4] Milgrom, M. *Astrophys. J.* **1983**, *270*, 365-370.

[5] Dodelson, S.; Liguori, M. *Phys. Rev. Lett.* **2006**, *97*, 23, 231301.

[6] Paczynski, B. *Astrophys. J.* **1986**, *304*, 1-5.

[7] Griest, K. *Astrophys. J.* **1991**, *366*, 412-421.

[8] Yoo, Y.; Chaname J.; Gould, A. *Astrophys. J.* **2004**, *601*, 311-318.

[9] Primack, J. R.; Seckel, D.; Sadoulet, B. *Annu. Rev. Nucl. Part. S.* **1988**, *38*, 751-807.

[10] Gunn, J. E.; Gott, J. R. *Astrophys. J.* **1972**, *176*, 1-19.

[11] Peebles, P. J. E. *The Large-Scale Structure of the Universe*; Princeton Univeristy Press: Princeton, NJ, USA, 1980.

[12] Springel, V.; White, S. D. M.; Jenkins, A.; Frenk, C. S.; Yoshida, N.; Gao, L.; Navarro, J.; Thacker, R.; Croton, D.; Helly, J. et al. *Nature* **2005**, *435*, 629-636.

[13] Klypin, A. A.; Kravtsov, A. V.; Valenzuela, O.; Prada, F. *Astrophys. J.* **1999**, *522*, 82-92.

[14] Navarro, J. F.; Frenk, C. S.; White, S. D.M. *Astrophys. J.* **1997**, *490*, 493-508.

[15] Weinberg, M. D.; Katz, N. *Astrophys. J.* **2002**, *580*, 627-633.

[16] Maccio, A. V.; Stinson, G.; Brook, C. B.; Wadsley, J.; Couchman, H. M. P.; Shen, S.; Gibso,n B. K.; Quinn, T. *Astrophys. J.* **2012**, *744*, L9.

[17] Zel'dovich, Ya. B. *Astron. Astrophys.* **1970**, *5*, 84-89.

[18] Ostriker, J. P.; Peebles, P. J. E.; Yahil, A. *Astrophys. J.* **1974**, *193*, L1-L4.

[19] Boyarsky, A.; Ruchayskiy, O.; Iakubovskyi, D. *J. Cosmol. Astropart. P.* **2009**, *3*, 5-26.

[20] Bulbul, E.; Markevitch, M.; Foster, A.; Smith, R. K.; Loewenstein, M.; Randall, S. W. *Astrophys. J.* **2014**, *789*, 13.

[21] Urban, O.; Werner, N.; Allen, S. W.; Simionescu, A.; Kaastra, J. S.; Strigari, L. E. *Mon. Not. R. Astron. Soc.* **2015**, *451*, 2447-2461.

[22] Boyarsky, A.; Ruchayskiy, O.; Iakubovskyi, D.; Franse, J. *Phys. Rev. Lett.* **2014**, *113*, 251301.

[23] Boyarsky, A.; Franse, J.; Iakubovskyi, D.; Ruchayskiy, O. *Phys. Rev. Lett.* **2015**, *115*, 161301.

[24] Jeltema, T. E.; Profumo, S. *Mon. Not. R. Astron. Soc.* **2015**, *450*, 2143-2152.

[25] Iakubovskyi, D. *Mon. Not. R. Astron. Soc.* **2015**, *453*, 4097-4101.

[26] Dodelson, S.; Widrow, L. M. *Phys. Rev. Lett.* **1994**, *72*, 17-20.

[27] Ruchayskiy, O. arXiv:0704.3215, 2007.

[28] Boyarsky, A.; Lesgourgues, J.; Ruchayskiy, O.; Viel, M. *Phys. Rev. Lett.* **2009**, *102*, 201304.

[29] Tremaine, S.; Gunn, J. E. *Phys. Rev. Lett.* **1979**, *42*, 407-410.

[30] Goerdt, T.; Moore, B.; Read, J. I.; Stadel, J.; Zemp, M. *Mon. Not. R. Astron. Soc.* **2006**, *368*, 1073-1077.

[31] Dolgov, A. D.; Hansen, S. H. *Astropart. Phys.* **2002**, *16*, 339-344.

[32] Adhikari, R.; Agostini, M.; Anh Ky, N.; Araki, T.; Archidiacono, M.; Bahr, M.; Baur, J.; Behrens, J.; Bezrukov, F.; Bhupal Dev, P. S. et. al *J. Cosmol. Astropart. P.* **2016**, 1602.04816.

[33] Asaka, T.; Blanchet, S.; Shaposhnikov, M. *Phys. Lett. B* **2005**, *631*, 151-156.

[34] Laine, M.; Shaposhnikov, M. *J. Cosmol. Astropart. P.* **2008**, *2008*, 031.

[35] Boyarsky, A.; Iakubovskyi, D.; Ruchayskiy, O. *Phys. Dark Universe* **2012**, *1*, 136-154.

[36] Klasen, M.; Pohl, M.; Sigl, G. *Prog. Part. Nucl. Phys.* **2015**, *85*, 1-32.

[37] Riemer-Sørensen, S. *Astron. Astrophys.* **2016**, *590*, A71.

[38] Boyarsky, A.; Ruchayskiy, O.; Shaposhnikov, M. *Annu. Rev. Nucl. Part. S.* **2009**, *59*, 191-214.

[39] Pal, P. B.; Wolfenstein, L. *Phys. Rev. D* **1982**, *25*, 766-773.

[40] Barger, V.; Phillips, R. J. N.; Sarkar, S. *Phys. Lett. B* **1995**, *352*, 365-371.

[41] Abazajian, K.; Fuller, G. M.: Tucker, W. H. *Astrophys. J.* **2001** *562*, 593-604.

[42] Boyarsky, A.; Neronov, A.; Ruchayskiy, O.; Shaposhnikov, M. *Mon. Not. R. Astron. Soc.* **2006**, *370*, 213-218.

[43] Mateo, M. *Annu. Rev. Astron. Astr.* **1998**, *36*, 435-506.

[44] Prokhorov, D. A.; Silk. J. *Astrophys. J.* **2010**, *725*, L131-L134.

[45] Chan, M. H. *Astrophys. Space Sci.*, **2016**, *361*, 116-121.